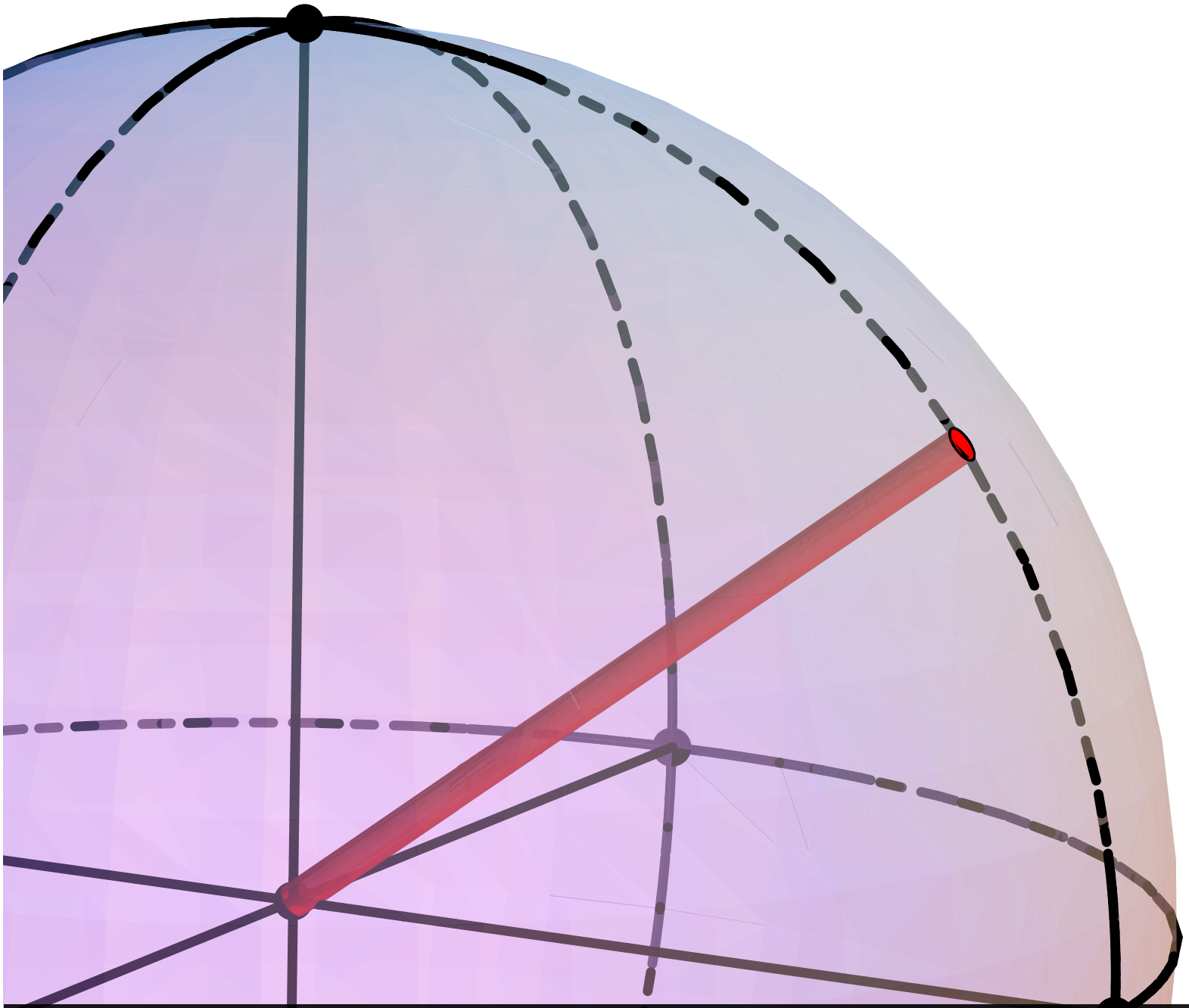

Quantum Computing with Majorana Fermions Coupled to Quantum Dots

Bjarke Mønsted & Monika Kovacic

May 27th, 2011

Bachelor's Thesis, Supervisor: Karsten Flensberg
Niels Bohr Institute, University of Copenhagen

Resumé

Dette projekt har til formål at diskutere mulige anvendelser af Majorana-fermioner i kvantecomputere. Efter indledningsvist at beskrive de vigtigste principper bag kvanteinformation og -computere, udleder vi den ikke-abelske statistik af Majorana-fermioner realiseret ved vortices i p-bølgesuperledere. Undervejs undersøger vi de effekter, som fører til denne statistisk, herunder fluxkvantisering og Aharonov-Bohm-effekten.

Efter udledningen undersøger vi en konkret model, hvori det er muligt at udføre visse logiske operationer på kvantebits i form af Majorana-fermioner koblet til kvantedots. Med baggrund i vores indledende afsnit om kvanteinformation, diskuterer vi styrker og svagheder ved modellen. Svaghederne inspirerer et par idéer til forbedringer, som vi redegør for vores overvejelser omkring.

Vi takker vores vejleder Karsten Flensberg og Morten Kjærgaard for al deres hjælp. Vi vil også sige tak til Anine, Esbilon og Lisa for rettelser og kage.

Endeligt en stor tak til vores rusvejledere for at give os en god start på fysikstudiet og for at introducere os til kvantefysik på den eneste rigtige måde.

Abstract

The topic of this bachelor's thesis is the application of Majorana fermions in quantum computers. We initially discuss important concepts of quantum information and quantum computation and later derive the non-abelian statistics of Majoranas realized as vortices in p-wave superconductors. We consider in details the effects leading to these statistics, including flux quantization and the Aharonov-Bohm effect.

We also consider a model for physical implementation of quantum bits using Majoranas coupled to quantum dots, which allows the construction of certain quantum gates. Based on our discussion of quantum information theory, we identify the weaknesses of the model, and examine in detail the possibility of improving it.

Monika Kovacic - 15/1-90

Bjarke Mønsted - 22/3-87

Contents

1 Introduction

The advantage of quantum computers over their classical counterparts stems in part from their ability to use bits in quantum mechanical superposition states, rather than just zero or one, in calculations. Unfortunately, many proposed realizations of these quantum bits, or *qubits*, are extremely vulnerable to decoherence, which destroys the superposition state.

Recently, this has motivated intense research into *topological quantum computers* - a term that covers models for quantum computing which are inherently protected against decoherence. In their realizations of qubits, these models use a type of quasiparticles known as *anyons*, which are characterized by their properties during interchanges. Whereas bosons and fermions pick up a phase factor of 1 and -1 from interchanges, these quasiparticles can pick up *any* phase – hence the name. This can lead to a property called *non-abelian statistics*, meaning that interchanges between different particles do not generally commute. Calculations are then performed by operations that interchange the anyons on a two-dimensional surface.

Such operations, known as *braiding*, can then be visualized as worldlines with two spatial and one temporal dimension. Since only the topology of the wordlines defines the calculations, and because slight perturbations do not affect this topology, the topological models of quantum computers are intrinsically fault-tolerant.

One kind of such anyons is *Majorana fermions*, or simply *Majoranas*, which is our main point of interest in this thesis. In the following, we give a brief overview of the structure of the thesis.

1.1 Overview

First, we will give a short introduction to quantum information and computation, which will introduce qubits and quantum gates and compare these with classical bits and gates. We also introduce the Bloch sphere representation of a single qubit, which will serve as a handy visualization of single-qubit states throughout the thesis. Following this, we give a brief introduction to the properties of Majorana fermions, which allows an in-depth discussion of their statistics.

Next, we investigate the rather exotic physical effects of realizing Majorana fermions as excitations in p-wave superconductors caused by a strong magnetic flux. We show that this magnetic flux must be quantized, and calculate the effects of the Aharonov-Bohm phase caused by the flux, which enables us to find expressions for the effects of braiding (cyclical interchanges) of Majoranas.

Using these expressions, we may finally derive 'braiding operators' that describe these interchanges. These operators will prove the non-abelian statistics of Majorana fermions, making them a strong candidate for topological quantum computing.

Having derived the non-abelian statistics of Majoranas, we consider a recently proposed model that implements Majoranas as qubits, and use charge controlled quantum dots to act as gates by causing single electrons to tunnel to or from the Majorana systems.

After describing this model, we discuss possible alterations to it and their consequences.

2 Quantum Computing

In the following, we will introduce the concepts of quantum bits, or *qubits*, and give examples of two types of quantum gates, which can act on the bits to perform various logical operations [1]. The realization of these gates is a natural goal for experimental quantum computing. For comparison, we will start off with a brief introduction to classical bits and gates.

2.1 Classical Bits and Gates

A classical bit can assume the logical values, or *truth values*, 0 and 1, and may be acted on by single-bit gates such as the NOT-gate, which 'flips' the value of the bit such that $0 \to 1$ and $1 \to 0$. Writing the set of possible bit values in curly brackets, we may then write

$$\{0, 1\} \xrightarrow{NOT} \{1, 0\}. \tag{2.1}$$

Multi-bit gates, on the other hand, act on multiple bits. An example is the AND-gate, which performs the transformations

$$\{00, 01, 10, 11\} \xrightarrow{AND} \{0, 0, 0, 1\}. \tag{2.2}$$

With this in mind, let us then look into the quantum analog.

2.2 Single Qubits

In quantum information theory, a qubit is defined as a vector in a two-dimensional complex vector space. Labelling a qubit state with $|\psi\rangle$, we may write

$$|\psi\rangle = \alpha|0\rangle + \beta|1\rangle, \tag{2.3}$$

where α and β are complex numbers and $|0\rangle$ and $|1\rangle$ correspond to the classical logical values of 0 and 1. We immediately notice that whereas classical bits only have two possible values, qubits can take any value given by the superposition in eq. (2.3) when not measured (although normalization puts some restrictions on the coefficients, which we will investigate later). The orthonormal basis spanned by the truth values of the bit, $|0\rangle$ and $|1\rangle$, is called the *computational basis*.

We also note that the probabilities of measuring 0 and 1, are $|\alpha|^2$ and $|\beta|^2$, respectively, so conservation of probability requires that

$$|\alpha|^2 + |\beta|^2 = 1 \tag{2.4}$$

at all times, which demands that all operators acting on $|\psi\rangle$ be unitary:

$$\hat{U}\hat{U}^\dagger = \hat{U}^\dagger\hat{U} = \mathbb{1}. \tag{2.5}$$

As unitary operators can change the state of a qubit into another, we can use unitary operators to construct quantum gates, to which we will dedicate sections 2.3 and 2.5. However, we will first introduce the Bloch sphere representation of qubits.

2.2.1 Bloch Sphere Representation

In most situations in physics, an intuitive way of visualizing the problem at hand is valuable. In this section, we arrive at a visual interpretation of single qubit states known as the *Bloch sphere representation*, which is also commonly used to describe spin.

Writing the complex coefficients in eq. (2.3) in polar coordinates, the expression becomes

$$|\psi\rangle = ze^{i\varphi_\alpha}|0\rangle + qe^{i\varphi_\beta}|1\rangle. \tag{2.6}$$

We may multiply this state by a global phase factor $e^{i\gamma}$, since measurable quantities, such as the expectation value of an operator $\hat{A}$, depend only on the squared moduli of the coefficents of the state:[1]

$$\langle \hat{A} \rangle = \langle \psi | e^{-i\gamma} \hat{A} e^{i\gamma} | \psi \rangle = \langle \psi | \hat{A} | \psi \rangle. \tag{2.7}$$

Thus, we may simplify (2.6) by multiplying with a global phase factor of $e^{-i\varphi_\alpha}$, and obtain

$$|\psi\rangle = z|0\rangle + qe^{i\varphi}|1\rangle, \tag{2.8}$$

where $\varphi = \varphi_\beta - \varphi_\alpha$. Writing the complex number $qe^{i\varphi}$ as $x+iy$, and recalling the normalization requirement from (2.4), we may write

$$z^2 + (x+iy)(x-iy) = x^2 + y^2 + z^2 = 1, \tag{2.9}$$

implying that possible values for x, y and z may be appropriately visualized as points on the surface of a unit sphere. Since surfaces only have two dimensions, we may eliminate our excess parameter by rewriting our coefficients in spherical coordinates with $r = 1$ using

$$\begin{aligned} x &= \cos\varphi \sin\theta', \\ iy &= i \sin\varphi \sin\theta', \\ z &= \cos\theta'. \end{aligned} \tag{2.10}$$

Our reason for denoting the zenith angle by θ' will become clear in a moment. This allows us to write the coefficients as

$$|\psi\rangle = z|0\rangle + (x+iy)|1\rangle = \cos\theta'|0\rangle + e^{i\varphi}\sin\theta'|1\rangle. \tag{2.11}$$

Since we would like opposite points on the Bloch sphere to represent orthogonal states, we investigate the results of a change of coordinates given by

$$(\theta', \phi) \to (\pi - \theta', \varphi + \pi) \tag{2.12}$$

changing $|\psi\rangle$ into $|\psi_{\text{opposite}}\rangle$:

$$\begin{aligned} |\psi_{\text{opposite}}\rangle &= \cos(\pi - \theta')|0\rangle + e^{i(\varphi+\pi)}\sin(\pi-\theta')|1\rangle \\ &= -\cos\theta'|0\rangle - e^{i\varphi}\sin\theta'|1\rangle \\ &= -|\psi\rangle. \end{aligned} \tag{2.13}$$

In the context of information theory, this is disasterous - if we assign to every Bloch vector a distinct information and if several vectors correspond to equivalent physical states, it will not be possible to determine from an experiment which piece of information our qubit is representing. We must make sure that every possible Bloch vector corresponds to one, and only one, physical state and vice versa, i.e. a bijective mapping.

Fortunately, we may 'spread out' our set of physical states across the whole sphere by setting $\theta' = \frac{\theta}{2}$ and thus restoring a bijective relation between physical states and Bloch sphere representations:

$$|\psi\rangle = \cos\left(\frac{\theta}{2}\right)|0\rangle + e^{i\varphi}\sin\left(\frac{\theta}{2}\right)|1\rangle, \tag{2.14}$$

where the qubit states $|0\rangle$ and $|1\rangle$ correspond to the north and south poles, respectively, as shown in figure 1. We can now verify that opposite points on the Bloch sphere correspond to orthogonal states by following the same procedure as in eq. (2.13) to obtain

$$|\psi\rangle = \cos\left(\frac{\theta}{2}\right)|0\rangle + e^{i\varphi}\sin\left(\frac{\theta}{2}\right)|1\rangle \to \tag{2.15}$$

$$|\psi_{\text{opposite}}\rangle = \sin\left(\frac{\theta}{2}\right)|0\rangle + e^{i(\varphi+\pi)}\cos\left(\frac{\theta}{2}\right)|1\rangle \tag{2.16}$$

[1] Phase *differences* can be observed through interference effects, but a global phase factor has no effect on the phase difference, so multiplying by a global phase gives us the same physical state.

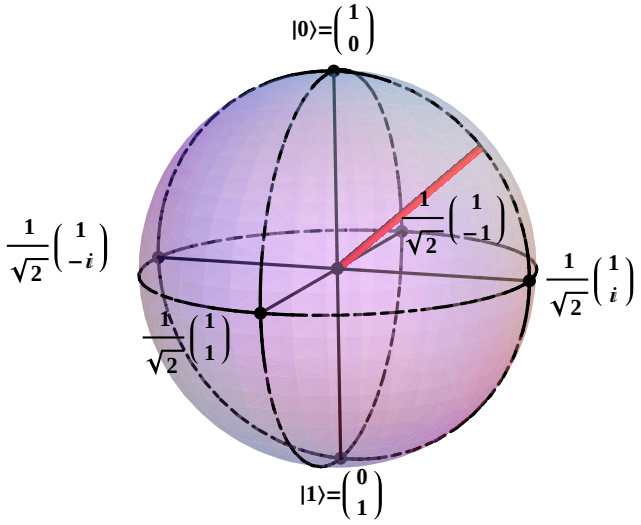

Figure 1: Bloch sphere representation of a qubit state represented by the red vector. The qubit states $|0\rangle$ and $|1\rangle$ are visualized as the north and south pole of the Bloch sphere.

finding

$$\langle\psi|\psi_{\text{opposite}}\rangle = \cos\left(\frac{\theta}{2}\right)\sin\left(\frac{\theta}{2}\right)\langle 0|0\rangle + e^{-i\varphi}e^{i(\varphi+\pi)}\sin\left(\frac{\theta}{2}\right)\cos\left(\frac{\theta}{2}\right)\langle 1|1\rangle \tag{2.17}$$

$$= \cos\left(\frac{\theta}{2}\right)\sin\left(\frac{\theta}{2}\right)\langle 0|0\rangle + e^{i\pi}\sin\left(\frac{\theta}{2}\right)\cos\left(\frac{\theta}{2}\right)\langle 1|1\rangle \tag{2.18}$$

$$= 0. \tag{2.19}$$

Having mapped all possible qubit states onto the surface of the Bloch sphere, the question is now how to describe the action of an unitary operator on the Bloch sphere. Let us look at single qubit gates.

2.3 Single-qubit Gates

Gates are active components that transform the state of a bit in a desired fashion. As a starting point let us consider the Pauli gates and seek to understand these transformations of a single qubit on the Bloch sphere.

2.3.1 Pauli Operators

Since a single qubit is a two-level quantum system, it can be convenient to treat it in the language of spin-half particles. Let us introduce the Pauli operators

$$\hat{\sigma}_x = \begin{bmatrix} 0 & 1 \\ 1 & 0 \end{bmatrix}, \hat{\sigma}_y = \begin{bmatrix} 0 & -i \\ i & 0 \end{bmatrix}, \hat{\sigma}_z = \begin{bmatrix} 1 & 0 \\ 0 & -1 \end{bmatrix}. \tag{2.20}$$

These matrices correspond to quantum gates and transform the state of a qubit $|\psi\rangle$ as

$$\begin{aligned}\hat{\sigma}_x \begin{pmatrix} \alpha \\ \beta \end{pmatrix} &= \begin{pmatrix} \beta \\ \alpha \end{pmatrix}, \\ \hat{\sigma}_y \begin{pmatrix} \alpha \\ \beta \end{pmatrix} &= \begin{pmatrix} -i\beta \\ i\alpha \end{pmatrix}, \\ \hat{\sigma}_z \begin{pmatrix} \alpha \\ \beta \end{pmatrix} &= \begin{pmatrix} \alpha \\ -\beta \end{pmatrix}.\end{aligned} \tag{2.21}$$

Note that $\hat{\sigma}_x$ corresponds to the classical NOT-gate, because it 'flips' the basis state:

$$\{|0\rangle, |1\rangle\} \xrightarrow{\hat{\sigma}_x} \{|1\rangle, |0\rangle\}. \tag{2.22}$$

However if we as an example apply the Pauli $\hat{\sigma}_x$ operation on the superposition state

$$\frac{1}{\sqrt{2}}\left(|0\rangle + |1\rangle\right) \xrightarrow{\hat{\sigma}_x} \frac{1}{\sqrt{2}}\left(|0\rangle + |1\rangle\right), \tag{2.23}$$

this just leaves the state unchanged.

Investigating the transformations of (2.21) on the Bloch sphere one realizes that the Pauli operators are equivalent to a reflection (or rotation by π) of the Bloch vector around the associated axis. This is visualized in figure 2.

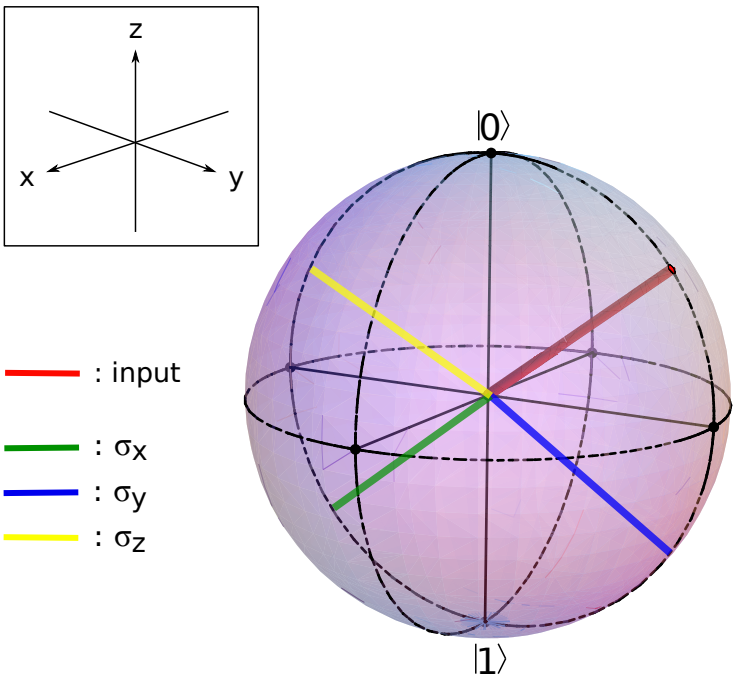

Figure 2: Bloch sphere representation of the rotations induced by the action of the Pauli matrices on the initial state (red vector). The action of $\{\hat{\sigma}_x, \hat{\sigma}_y, \hat{\sigma}_z\}$ transforms the inital state (red) to a new state represented by the {green, blue, yellow} vector, respectively. So, the action of the Pauli matrices correspond to π-rotation of the Bloch vector around the associated axis.

2.3.2 Rotation Operators

It can be shown [1, p. 175] that in general, a rotation by ϕ around an axis $\hat{n} = (n_x, n_y, n_x)$ is given by

$$R_{\hat{n}}(\phi) \equiv e^{i\phi\hat{n}\cdot\boldsymbol{\sigma}/2} = \cos(\frac{\phi}{2})\hat{\mathbb{1}} - i\sin(\frac{\phi}{2})(n_x\hat{\sigma}_x + n_y\hat{\sigma}_y + n_z\hat{\sigma}_z), \tag{2.24}$$

where $\boldsymbol{\sigma} = (\hat{\sigma}_x, \hat{\sigma}_y, \hat{\sigma}_z)$, and we use that $(\hat{n}\cdot\boldsymbol{\sigma})^2 = \hat{\mathbb{1}}$. This rotation operator will play an important role since any unitary transformation can be decomposed into a rotation on the Bloch sphere multiplied by a global phase [1, p. 175]:

$$\hat{U} = e^{i\alpha}R_{\hat{n}}(\phi), \tag{2.25}$$

where α, ϕ and the three-dimensional unit vector $\hat{n}$ are real. This is a nice feature, as we can now visulize any single-qubit gate as a rotation on the Bloch sphere.

2.3.3 Hadamard, Phase and $\pi/8$ Gate

In this short section, we introduce three single-qubit gates which are not very prominent in this thesis, but nevertheless play an important role in the subject of universal quantum computation, which will be discussed at the end of this chapter.

First, let $\alpha = \pi/2$, $\phi = \pi$ and $\hat{n} = (\frac{1}{\sqrt{2}}, 0, \frac{1}{\sqrt{2}})$ in eq. 2.25 to obtain a transformation known as the *Hadamard gate*:

$$\begin{aligned}\hat{U} &= e^{i\pi/2}R_{\hat{n}}(\pi) && (2.26)\\ &= e^{i\pi/2}\left[\cos(\pi/2)\hat{\mathbb{1}} - i\sin(\pi/2)\frac{1}{\sqrt{2}}(\hat{\sigma}_x + \hat{\sigma}_z)\right] && (2.27)\\ &= \frac{1}{\sqrt{2}}\begin{bmatrix}1 & 1\\ 1 & -1\end{bmatrix} \equiv H, && (2.28)\end{aligned}$$

Note, that the Hadamard gate can be obtained form the Pauli operators as $H = (\hat{\sigma}_x + \hat{\sigma}_z)/\sqrt{2}$ and that it transforms a qubit in the computation basis as

$$H\begin{pmatrix}\alpha\\ \beta\end{pmatrix} = \frac{1}{\sqrt{2}}\begin{pmatrix}\alpha+\beta\\ \alpha-\beta\end{pmatrix}. \tag{2.29}$$

The phase and $\pi/8$ gates, denoted S and T, on the other hand induce rotations by $\pi/2$ and $\pi/4$ around the z-axis, which we can write as

$$S \equiv \begin{bmatrix}1 & 0\\ 0 & i\end{bmatrix} = e^{i\pi/4}\begin{bmatrix}e^{-i\pi/4} & 0\\ 0 & e^{i\pi/4}\end{bmatrix} = e^{i\pi/4}R_z(\pi/2), \tag{2.30}$$

$$T \equiv \begin{bmatrix}1 & 0\\ 0 & e^{i\pi/4}\end{bmatrix} = e^{i\pi/8}\begin{bmatrix}e^{-i\pi/8} & 0\\ 0 & e^{i\pi/8}\end{bmatrix} = e^{i\pi/8}R_z(\pi/4). \tag{2.31}$$

Now we have seen that the action of single-qubit gates induces a rotation on the Bloch sphere.

2.4 Multiple Qubits

Just as in classical computing, we need to consider the state of n qubits. This is written as the tensor product of n qubit states

$$|\psi\rangle_n = |\psi_1\rangle \otimes |\psi_1\rangle \otimes \cdots \otimes |\psi_n\rangle. \tag{2.32}$$

In general, a system of n qubits is a 2^n-level system with 2^n basis states. In the case of two qubits, the computational basis is

$$\{|00\rangle, |01\rangle, |10\rangle, |11\rangle\} \tag{2.33}$$

We write a single-qubit gate U acting only on the jth qubit as $U^{(j)}$. The action of this gate is

$$U^{(j)}|\psi\rangle_n = |\psi_1\rangle \otimes \cdots \otimes (U|\psi_j\rangle) \otimes \cdots \otimes |\psi_n\rangle. \tag{2.34}$$

As an example, consider the action of the Pauli operator $\hat{\sigma}_x$ on the first of the two qubits in the multi-qubit state $|10\rangle$:

$$\hat{\sigma}_x|1\rangle \otimes \hat{\mathbb{1}}|0\rangle = |00\rangle \tag{2.35}$$

In the following section we introduce *multi-qubit gates*, which transform both of the qubit subspaces.

2.5 Controlled Multi-qubit Gates

A type of multi-qubit gate of particular interest is the controlled gate, which acts on a control qubit $|c\rangle$ and a target qubit $|t\rangle$, transforming only the state of the target qubit. Denoting initial and final states by i and f, we write

$$|c_i\rangle|t_i\rangle \xrightarrow{\hat{U}_C} |c_i\rangle|t_f\rangle, \tag{2.36}$$

meaning "If $|c\rangle$ is true ($|1\rangle$), then and only then apply U to $|t\rangle$".

In the computational basis, (2.33), this is a block diagonal 4×4 matrix of the form

$$\hat{U}_c = |0\rangle\langle 0| \otimes \hat{\mathbb{1}} + |1\rangle\langle 1| \otimes \hat{U} = \left[\begin{array}{cc|cc} 1 & 0 & 0 & 0 \\ 0 & 1 & 0 & 0 \\ \hline 0 & 0 & U_{11} & U_{12} \\ 0 & 0 & U_{21} & U_{22} \end{array}\right]. \tag{2.37}$$

A useful control gate is the controlled-NOT or CNOT:

$$\hat{U}_{CNOT} = |0\rangle\langle 0| \otimes \mathbb{1} + |1\rangle\langle 1| \otimes \hat{\sigma}_x. \tag{2.38}$$

The matrix representation in the computational basis:

$$\hat{U}_{CNOT} = \begin{bmatrix} 1 & 0 & 0 & 0 \\ 0 & 1 & 0 & 0 \\ 0 & 0 & 0 & 1 \\ 0 & 0 & 1 & 0 \end{bmatrix}. \tag{2.39}$$

Looking at the columns of this matrix, we see that it transforms two-qubit states in the following way:

$$\{|00\rangle, |01\rangle, |10\rangle, |11\rangle\} \xrightarrow{\hat{U}_{CNOT}} \{|00\rangle, |01\rangle, |11\rangle, |10\rangle\}. \tag{2.40}$$

So, if our control qubit is set to $|1\rangle$, then the NOT-gate, $\hat{\sigma}_x$, is applied to the target qubit.

At this point, we have examined fundamental gates and it is natural to wonder how many gates we have to construct to be capable of performing any desired quantum computation. This is the subject of *universality*.

2.6 Universality

In the following, we wish to introduce the notions of *universal quantum computation* and *universal sets of single-qubit gates*. Distinguishing between these terms is important, so we will introduce them seperately.

Universal Sets of Single-Qubit Gates

This term covers a set of single-qubit gates which can transform a given single-qubit state into any other single-qubit state. As an example, we show that the set of gates consisting of two rotation operators around different axes, with tunable angle, is universal.

The simple, but not very rigorous, way of showing this is to refer to the Bloch sphere illustration in figure 1. From the figure, it can be seen that if we may rotate the Bloch vector with angles of our choosing around two set non-parallel axes, we may reach any point on the sphere. The proof is rather cumbersome, so we choose to omit it.

Universal Quantum Computing

This term refers to the ability of a set of gates to *approximate any unitary transformation to arbitrary accuracy*, meaning that any quantum computation is possible on the set of gates in question. It has been proven that the Hadamard, phase, $\pi/8$- and CNOT-gates constitute such a set[1, pp. 188-194]. We do not replicate the proof here, but merely state the result as motivation for our attempts to arrive at physical realizations of controlled gates and universal single-qubit sets (with which we may then construct the Hadamard phase and $\pi/8$ gates).

3 Majorana Fermions

The theoretical concept of the Majorana fermion was introduced in the 1930's by Ettore Majorana, and have become interesting over recent years as they may be realized experimentally as quasiparticle excitations in superconductors[2, 247-51]. Mathematically, Majorana fermions, or simply Majoranas, are descriped by superpositions of fermionic creation and annihilation operators, so before we discuss the properties of Majoranas and derive their statistics, we briefly review the properties of fermionic operators.

3.1 Fermionic operators

This section deals with the fermionic *creation* and *annihilation operators* known from the formalism of second quantization. The operators are denoted $\hat{c}^\dagger$ and $\hat{c}$, respectively, and their effects can be qualitatively described as adding and removing a fermion to a given system state. More accurately, we may write

$$\begin{aligned} \hat{c}^\dagger|0\rangle &= |1\rangle, \\ \hat{c}|1\rangle &= |0\rangle, \\ \hat{c}^\dagger|1\rangle &= 0, \\ \hat{c}|0\rangle &= 0. \end{aligned} \tag{3.1}$$

As we will show later on, $|0\rangle$ and $|1\rangle$ are the only allowed states for fermionic systems.

$\hat{c}$ and $\hat{c}^\dagger$ obey the following relations

$$\begin{aligned} \hat{c}\hat{c} = \hat{c}^\dagger\hat{c}^\dagger &= 0, \\ \{\hat{c}_n^\dagger, \hat{c}_m^\dagger\} &= 0, \\ \{\hat{c}_n, \hat{c}_m^\dagger\} &= \delta_{nm} \Rightarrow \\ [\hat{c}, \hat{c}^\dagger] &= 1 - 2\hat{c}^\dagger\hat{c}, \end{aligned} \tag{3.2}$$

where curly brackets denote anticommutators, i.e. $\hat{c}\hat{c}^\dagger + \hat{c}^\dagger\hat{c} = 1$, for instance. Furthermore, we know from basic quantum mechanics that the number states, $|n\rangle$, are eigenstates of the number operator $\hat{n} = \hat{c}^\dagger\hat{c}$ with

$$\hat{c}^\dagger\hat{c}|n\rangle = n|n\rangle, \tag{3.3}$$

and form a complete set

$$\sum_n |n\rangle\langle n| = \mathbb{1}. \tag{3.4}$$

However, rewriting the squared number operator $\hat{n}^2 = \hat{c}^\dagger\hat{c}\hat{c}^\dagger\hat{c}$ using the relations in (3.2) yields

$$\hat{n}^2 = \hat{c}^\dagger(1 - \hat{c}^\dagger\hat{c})\hat{c} = \hat{c}^\dagger\hat{c} = \hat{n}. \tag{3.5}$$

Evidently, the states must satisfy $n = n^2$, i.e., the only allowed states are $n = 0, 1$. This means that, for an arbitrary state $|\Psi\rangle$, we can use (3.4) to write out the mathematically trivial, but physically interesting, expression $|\Psi\rangle = \mathbb{1}|\Psi\rangle$ and obtain

$$|\Psi\rangle = \sum_n |n\rangle\langle n|\Psi\rangle, \tag{3.6}$$

$$= c_0|0\rangle + c_1|1\rangle, \tag{3.7}$$

which has the same form as the state of a qubit (2.3) indicating that we may use the fermionic number states to define a qubit.

3.2 Properties of Majorana Fermions

One consideration which leads to a description involving Majorana fermions arises when attempting to write the fermionic creation and annihilation operators $\hat{c}$ and $\hat{c}^\dagger$ as

$$\hat{c} = (\gamma_1 + i\gamma_2)/2, \tag{3.8}$$

$$\hat{c}^\dagger = (\gamma_1 - i\gamma_2)/2, \tag{3.9}$$

where γ_1 and γ_2 are the Majorana operators. By adding or subtracting eqs. (3.8) and (3.9), the following expressions for γ_1 and γ_2 can be obtained:

$$\begin{aligned} \gamma_1 &= \hat{c}^\dagger + \hat{c}, \\ \gamma_2 &= i(\hat{c}^\dagger - \hat{c}). \end{aligned} \tag{3.10}$$

From the definitions in eqs. (3.10) and the properties of fermionic operators summarized in eqs. (3.2), it is easily seen that the Majorana operators satisfy

$$\gamma_i^\dagger = \gamma_i \tag{3.11}$$

and

$$\gamma_i^2 = \hat{c}\hat{c}^\dagger + \hat{c}^\dagger\hat{c} = \{\hat{c}, \hat{c}^\dagger\} = 1. \tag{3.12}$$

Unitarity, then, follows from the expressions above, as $\gamma_i^\dagger\gamma_i = \gamma_i^2 = 1$. The anticommutator $\{\gamma_i, \gamma_j\}$ can be calculated using (3.12) for $i = j$ and (3.10) for $i \neq j$:

$$\{\gamma_i, \gamma_j\} = \gamma_i\gamma_j + \gamma_j\gamma_i = 2\gamma_i^2 = 2 \qquad \text{if } i = j, \tag{3.13}$$

$$\{\gamma_i, \gamma_j\} = \gamma_i\gamma_j + \gamma_j\gamma_i = \gamma_i\gamma_j - \gamma_i\gamma_j = 0 \qquad \text{if } i \neq j. \tag{3.14}$$

For later purposes, it is rewarding to use the anticommutator for i and $i + 1$ to show that

$$(\gamma_{i+1}\gamma_i)^2 = \gamma_{i+1}\gamma_i\gamma_{i+1}\gamma_i = -\gamma_{i+1}^2\gamma_i^2 = -1 \tag{3.15}$$

The relevant properties of the Majorana fermions can then be summarized as

$$\begin{aligned} \gamma_i^\dagger &= \gamma_i, \\ \gamma_i^2 &= 1, \\ \{\gamma_i, \gamma_j\} &= 2\delta_{ij}, \\ (\gamma_{i+1}\gamma_i)^2 &= -1. \end{aligned} \tag{3.16}$$

4 Braiding Statistics

The purpose of this chapter is to show that Majorana fermions have *non-abelian braiding statistics*, a term which concerns the effects of an interchange of two particles. Majorana interchanges do *not* generally commute, as opposed to interchanges of ordinary fermions and bosons, which get a phase factor of -1 and 1, respectively. Because this factor is independent of which particles are interchanged, we may say that interchanges in bosonic and fermionic systems commute, i.e. they have abelian statistics.

In general, our approach follows that of a recent article by Ivanov [3]. However, we derive in detail the 'transformation rules', which serve as a premise in Ivanov's work. Our procedure will be to derive an expression for the Aharonov-Bohm, or AB, phase acquired by a Majorana fermion during interchanges. This AB phase, however, depends on the magnetic flux through the superconductor (which is quantized, as we will show), so we must first examine the properties of superconductors and their response to magnetic fluxes.

A Few Properties of superconductors

Although interesting in their own right, superconductors are not a central topic in this thesis, and will not be treated in-depth. We will merely give a short description of the concepts of *Cooper pairs* and *vortices*, which are important to our derivations, and refer the reader to relevant litterature[4].

Cooper-pairing is the abilty of a large number of electrons to form a condensate of pairs which is descriped by a single wavefunction. We may write this in polar coordinates as

$$\Psi_S(\mathbf{r}, \theta) = |\Delta| e^{i\theta(\mathbf{r})}, \tag{4.1}$$

where Δ is known as the *BCS gap parameter*. eq. (4.1) will play an important role in the derivation of flux quantization.

Vortices in superconductors are circulating currents that form in order to cancel out applied magnetic fields. As shown in figure 3, a vortex will be formed near each applied magnetic field. As the distance from the center of an applied flux becomes large, the magnetic field, and thus

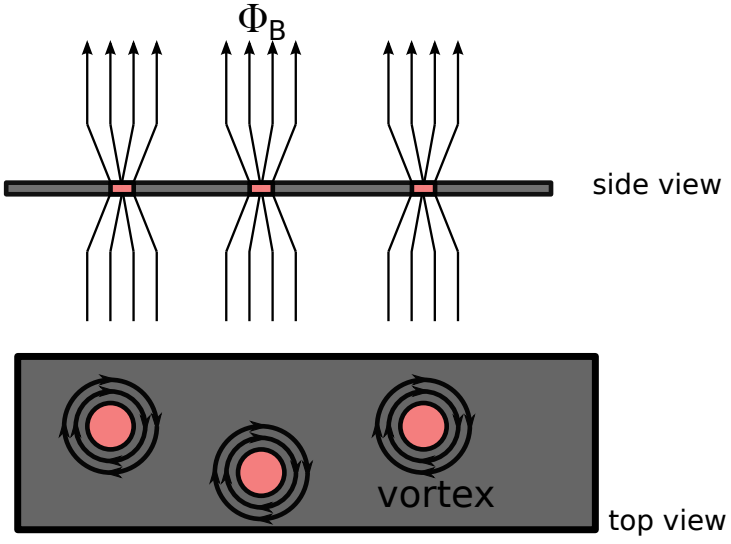

Figure 3: Illustration of vortices in a 2D superconductor

the current required to cancel it, vanishes, so we expect the vortices to be localized near each

applied flux.[2] Taking these two effects as a premise, we may derive the effect of quantization of fluxes applied to superconductors.

4.1 Flux Quantization

The purpose of this section is to argue that the magnetic flux through a vortex in a p-wave superconductor is quantized, as proving this is essential to our discussion of the effects of Majorana braiding.

We first consider a condensate wavefunction in the form of eq. (4.1). At a large distance R from a vortex at the origin, no current is expected to run. In the presence of a vector potential $\mathbf{A}(\mathbf{r})$, the canonical momentum operator $\hat{p} = -i\hbar\nabla$ gets an extra term, so the new operator $\hat{p}'$ is

$$\hat{p}' = -i\hbar\nabla - q\mathbf{A}(\mathbf{r}). \tag{4.2}$$

Thus, the expression for the current at distance R from the vortex is

$$J(\mathbf{r}) = \Psi_S^*(\mathbf{r})\frac{1}{m}\left(\frac{\hbar}{i}\nabla - q\mathbf{A}(\mathbf{r})\right)\Psi_S(\mathbf{r}), \tag{4.3}$$

$$= \frac{|\Psi_S(\mathbf{r})|^2}{m}\left(\hbar\nabla\theta(\mathbf{r}) - q\mathbf{A}(\mathbf{r})\right), \tag{4.4}$$

$$= 0, \tag{4.5}$$

from which it is easy to see that $\hbar\nabla\theta(\mathbf{r}) = q\mathbf{A}(\mathbf{r})$. A circular path integral on both sides yields

$$\hbar\oint \nabla\theta(\mathbf{r})\cdot \mathrm{d}\mathbf{l} = q\oint \mathbf{A}(\mathbf{r})\cdot \mathrm{d}\mathbf{l}. \tag{4.6}$$

We require azimuthal periodicity in (4.1), so the LHS is $2\pi n\hbar$, whereas the RHS can be rewritten using Stokes' theorem:

$$q\oint \mathbf{A}(\mathbf{r})\cdot \mathrm{d}\mathbf{l} = q\int \underbrace{(\nabla\times\mathbf{A}(\mathbf{r}))}_{=\mathbf{B}}\cdot \mathrm{d}\mathbf{a}, \tag{4.7}$$

$$= q\Phi, \tag{4.8}$$

where we identified the magnetic flux $\Phi = \int \mathbf{B}\cdot d\mathbf{a}$. Notice that $\nabla\times\mathbf{A}$ is only assumed to be zero along the integration path, and so we expect a nonzero magnetic flux because the surface integral includes regions with a non-vanishing magnetic field, that is $\nabla\times\mathbf{A} \neq 0$.
The quantization of the magnetic flux can now be expressed as

$$\Phi = \frac{2\pi n\hbar}{q}, \tag{4.9}$$

where n is the flux quantum number.

To see how this affects the braiding of Majorana fermions, we must investigate the Aharonov-Bohm effect in the case of an electromagnetic vector potential arising from a quantized magnetic flux.

4.2 The Aharonov-Bohm Phase

This section is intended to demonstrate how, given a solution Ψ to the Schrödinger equation, a new solution Ψ' to a Schrödinger equation including a vector potential term can be obtained. We first consider an arbitrary curlless, vector potential, and move on to treat the special case of the vector potential caused by a quantized magnetic flux.

[2] For a detailed treatment of these effects, see *Phillips*[2]

In the presence of an electromagnetic potential, the canonical momentum operator is given by (4.2), and results in the Schrödinger equation

$$i\hbar\frac{\partial\Psi}{\partial t} = \frac{1}{2m}\left(\frac{\hbar}{i}\nabla - q\mathbf{A}\right)^2\Psi + V\Psi. \tag{4.10}$$

Observing that the RHS of (4.10) contains zeroth, first and second order spatial derivative terms of Ψ is an excellent motivation to try a few calculatory tricks. A trick for solving differential equations like this in regions where $\nabla\times\mathbf{A}=0$ (which must be the case if our discussion from section 4.1 is to apply), is to attempt to collect the terms in the parenthesis on the RHS of (4.10), by defining Ψ' such that

$$\Psi = \Psi'\exp\left(\frac{qi}{\hbar}\int_{\mathbf{0}}^{\mathbf{r}}\mathbf{A}(\mathbf{r}')\cdot d\mathbf{r}'\right), \tag{4.11}$$

setting $g(\mathbf{r}) \equiv \frac{q}{\hbar}\int_{\mathbf{0}}^{\mathbf{r}}\mathbf{A}(\mathbf{r}')\cdot d\mathbf{r}'$. Calculating $\hat{p}\,\Psi$, and exploiting that $\nabla g(\mathbf{r}) = (q/\hbar)\mathbf{A}(\mathbf{r})$ yields

$$\begin{aligned}\frac{\hbar}{i}\nabla\Psi &= \frac{\hbar}{i}\nabla\left(e^{ig(\mathbf{r})}\Psi'\right)\\ &= \frac{\hbar}{i}\big(i\nabla g(\mathbf{r})\big)e^{ig(\mathbf{r})}\Psi' + \frac{\hbar}{i}e^{ig(\mathbf{r})}\nabla\Psi'\\ &= q\mathbf{A}(\mathbf{r})\Psi + \frac{\hbar}{i}e^{ig(\mathbf{r})}\nabla\Psi'\end{aligned} \tag{4.12}$$

This effectively turns eq. (4.10) into a second order differential equation as $-i\hbar\nabla\Psi = (-i\hbar\nabla + q\mathbf{A})\Psi'$, so the momentum term in (4.10) becomes

$$\left(\frac{\hbar}{i}\nabla - q\mathbf{A}\right)\Psi = \frac{\hbar}{i}(\nabla\Psi')e^{ig(\mathbf{r})}, \tag{4.13}$$

and thus

$$\left(\frac{\hbar}{i}\nabla - q\mathbf{A}\right)^2\Psi = -\hbar^2 e^{ig(\mathbf{r})}\nabla^2\Psi'. \tag{4.14}$$

By insertion in (4.10), Ψ' satisfies the ordinary Schrödinger equation, meaning that the solution to the Schrödinger equation in the presence of a curlless vector potential is just the ordinary solution multiplied by $\exp(\frac{qi}{\hbar}\int_{\mathbf{o}}^{\mathbf{r}}\mathbf{A}(\mathbf{r}')\cdot d\mathbf{r}')$, that is, introducing $\mathbf{A}(\mathbf{r})$ into the Scrödinger equation leads to a transformation in a given solution Ψ given by

$$\Psi \to \Psi\exp\left(\frac{qi}{\hbar}\int_{\mathbf{0}}^{\mathbf{r}}\mathbf{A}(\mathbf{r}')\cdot d\mathbf{r}'\right) = \Psi\cdot e^{ig(\mathbf{r})}. \tag{4.15}$$

Moving on now to the special case of a vector potential caused by a quantized magnetic flux, we recall from our discussion of (4.8) that

$$\Phi = \oint\mathbf{A}\cdot\mathrm{d}\mathbf{l} = \int(\nabla\times\mathbf{A})\cdot\mathrm{d}\mathbf{a}, \tag{4.16}$$

in regions far from the vortex. Due to gauge invariance, we may perform a transformation $\mathbf{A}\to\mathbf{A}+\nabla\Lambda$ to the Coulomb gauge, such that $\nabla\cdot\mathbf{A}=0$. In that case, and choosing a circular path in the LHS of (4.16), we can set $\mathbf{A}$ parallel to $\mathrm{d}\mathbf{l}$ and write

$$\mathbf{A}(\mathbf{r}) = A_r(\mathbf{r})\cdot\hat{\boldsymbol{r}} + A_\phi(\mathbf{r})\cdot\hat{\boldsymbol{\phi}} \tag{4.17}$$

$$= A_\phi(r)\cdot\hat{\boldsymbol{\phi}}. \tag{4.18}$$

Now, with no radial component in $\mathbf{A}$ and only a scalar radial dependency in its azimuthal component, eq. (4.16) becomes

$$\Phi = \oint\mathbf{A}(\mathbf{r})\cdot\mathrm{d}\mathbf{l} = \int_0^{2\pi}A_\phi(r)r\,\mathrm{d}\phi \tag{4.19}$$

$$= 2\pi r A_\phi(r)\Rightarrow, \tag{4.20}$$

$$\mathbf{A} = \frac{\Phi}{2\pi r}\hat{\boldsymbol{\phi}}, \tag{4.21}$$

where the flux is given by (4.9). Notice that a path integral over any trajectory for $\mathbf{A}$ will depend only on the azimuthal angle ϕ. Thus, we may obtain an expression for the Aharonov-Bohm phase, caused by a rotation of an arbitrary angle around a vortex, from (4.15). For a single flux quantum ($n = 1$), this is

$$\Psi \to \Psi \exp\left(\frac{qi}{\hbar}\int_{\mathbf{0}}^{\theta}\frac{n\hbar}{qr}r\,\mathrm{d}\phi\right) \Rightarrow \tag{4.22}$$

$$\Psi' = \Psi \exp\left(i\theta\right). \tag{4.23}$$

In the following, we will investigate the effects of this phase in the presences of several vortices, and how this affects the interchange of vortices, which will finally allow us to derive the braiding operators.

4.3 Transformation Rules

Because vector fields are additive, we can calculate the general expression for the phase in the presence of multiple vortices at positions $\mathbf{R}_n$:

$$\Psi' = \Psi \exp\left(i\sum_n \theta_n\right) = \Psi \exp\left(i\sum_n \arg\left(\mathbf{r}-\mathbf{R}_n\right)\right). \tag{4.24}$$

These phases are illustrated in figure 4.

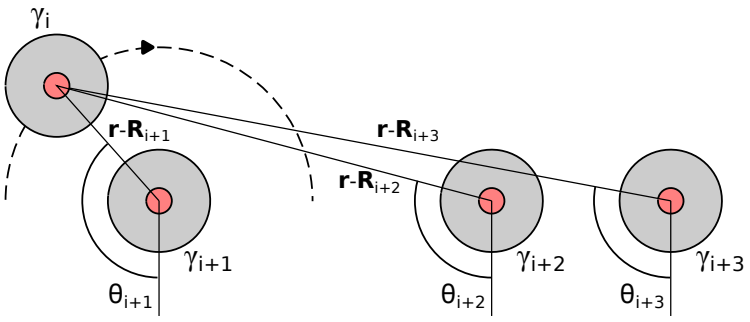

Figure 4: Illustration of the phase shift arising from moving one vortex around another.

It can be shown[7] that the zero energy solution to the Bogolubov-de-Gennes equations at each vortex is a Majorana fermion, and can be written as

$$\gamma = \frac{1}{\sqrt{2}}\int \mathrm{d}r\left(F(\mathbf{r})e^{-i\Omega/2}\hat{c} + h.c.\right), \tag{4.25}$$

where $F(\mathbf{r})$ is an envelope function that localizes the Majorana and

$$\Omega = \sum_n \arg\left(\mathbf{r}-\mathbf{R}_n\right). \tag{4.26}$$

Thus the mth Majorana is described by

$$\gamma_m = \frac{1}{\sqrt{2}}\int \mathrm{d}r\left(F(\mathbf{r})e^{-i\Omega_m/2}\hat{c} + h.c.\right), \tag{4.27}$$

where

$$\Omega_m = \sum_{n\neq m} \arg\left(\mathbf{r}-\mathbf{R}_n\right). \tag{4.28}$$

It can be seen that γ_m has branch points in all coordinates given by $\mathbf{R}_n$, because all transformations of the type $\theta_n \to \theta_n + 2\pi$ lead to the changes in γ_m given by $\gamma_m \to -\gamma_m$. Note, however, that a change of 4π in θ_n gives no change in γ.[3] Thus, single valuedness can be restored by introducing branch cuts (see figure 5) from each vortex such that the phase change when moving vortex m an arbitrary angle around vortex n (for simplicity, we start at $\theta = 0$) is $\theta_n + 2l\pi$, where l is the number of times the branch cut has been crossed. In terms of γ_m,

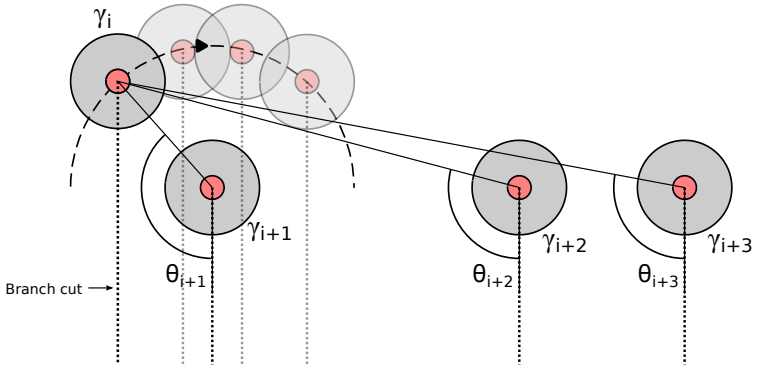

Figure 5: Graphical representation of the branch cuts (dashed lines). The mth Majorana can now be taken as one single valued function $\gamma_m(\theta_1, \theta_2, ..., \theta_n)$ before crossing the cut, and as a new single valued function $-\gamma_m(\theta_1, \theta_2, ..., \theta_n)$ after crossing the cut.

then, this is equivalent to the change given by

$$\gamma_m(\theta = 0) \to (-1)^l \gamma_m(\theta_n), \tag{4.29}$$

In order to investigate the effects of an interchange of two neighbouring Majoranas, we now introduce an operator T_i, which exchanges the ith Majorana with the $(i+1)$th. From figure 5 we see that γ_i does not cross a branch cut, and so, relabelling the Majoranas after the interchange, we have the transformation

$$\gamma_i \to \gamma_{i+1}. \tag{4.30}$$

The other Majorana involved in the exchange, however, crosses the one cut originating from γ_i, and so eq. (4.29) gives us the transformation

$$\gamma_{i+1} \to -\gamma_i. \tag{4.31}$$

We also note that the Majoranas that are not involved in the exchange cross either zero, or an even number of branch cuts., Using (4.29) we may conclude, that the phase of the remaining Majoranas is unchanged. So to sum up, the transformation rules are

$$\begin{aligned} T_i(\gamma_i) &= \gamma_{i+1}, \\ T_i(\gamma_{i+1}) &= -\gamma_i, \\ T_i(\gamma_j) &= \gamma_j, \end{aligned} \tag{4.32}$$

where $j \neq i, i+1$.

4.4 Derivation of the Braiding Operators

Having obtained the transformation rules, we may begin our search for unitary operators which describe the same interchanges, that is, we seek a unitary operator τ_i, such that

$$T_i(\gamma_j) = \tau_i \gamma_j \tau_i^{-1}. \tag{4.33}$$

[3] Functions of the type $z^{1/2}$, where z is a complex number, are often used as a textbook example of branch points in contour integral theory - see for instance Riley[6, p. 721]

In the following, we will see that this can be realized by defining

$$\tau_i^{\pm 1} = \frac{1}{\sqrt{2}}(1 \pm \gamma_{i+1}\gamma_i). \tag{4.34}$$

Using the anticommutator from (3.16), it can be shown that (4.34) is unitary:

$$\tau_i \tau_i^{-1} = (1 + \gamma_{i+1}\gamma_i)(1 - \gamma_{i+1}\gamma_i)/2 = (1 - \gamma_{i+1}\overbrace{\gamma_i\gamma_{i+1}}^{=-\gamma_{i+1}\gamma_i}\gamma_i)/2, \tag{4.35}$$

$$= 1. \tag{4.36}$$

It can now be checked whether the transformation described by (4.34) obeys the rules of eqs. (4.32) in the three relevant cases, i.e. whether $\tau_i\gamma_j\tau_i^{-1} = T_i(\gamma_j)$ for $j = i$, $j = i+1$ and $j \neq i, i+1$, respectively, which can be be verified using the relation summarized in eqs. (3.16).

4.5 Exponential Form

In the following, we will show that (4.34) can also be written in the form of an exponential as

$$\exp(\pi/4\,\hat{O}) = \frac{1}{\sqrt{2}}(1 \pm \hat{O}), \tag{4.37}$$

where we define $\hat{O} \equiv (\gamma_{i+1}\gamma_i)$ for simplicity.

Before moving on, we would like to point out the analogy to Eulers famous identity

$$e^{i\theta} = \cos\theta + i\sin\theta. \tag{4.38}$$

This identity is usually proved by writing out the Taylor series of $e^{i\theta}$, where the alternating sign in the series for $\sin\theta$ and $\cos\theta$ is ensured because $i^2 = -1$. This is analogous to $\hat{O}^2 = -\mathbb{1}$, which is ensured by eq. (3.16). Thus, it seems appropriate to write out the Taylor series for eq. (4.37):

$$\exp\left(\frac{\pi}{4}\hat{O}\right) = \sum_{n=0}^{\infty} \frac{\hat{O}^n}{n!} \nabla^n \exp\left(\frac{\pi}{4}\hat{O}\right)\Big|_0, \tag{4.39}$$

$$= \sum_{n=0}^{\infty} \frac{\hat{O}^n}{n!}\left(\frac{\pi}{4}\right)^n, \tag{4.40}$$

where $\nabla^n = \dfrac{\partial^n}{\partial \hat{O}^n}$.

From (3.16) we know that $\hat{O}^2 = -\mathbb{1}$, so

$$\hat{O}^{2n} = (-\mathbb{1})^n. \tag{4.41}$$

It now seems apropriate to let our derivation follow the structure of a Taylor series-based proof for Eulers famous identity. Using the same approach on the odd integers $(2n+1)$ yields

$$\hat{O}^{2n+1} = \hat{O}^{2n}\hat{O}, \tag{4.42}$$

$$= (-1)^n\hat{O}. \tag{4.43}$$

Equation (4.40) can now be rewritten as

$$\exp\left(\frac{\pi}{4}\hat{O}\right) = \sum_{n=0}^{\infty} \frac{\hat{O}^n}{n!}\left(\frac{\pi}{4}\right)^n, \tag{4.44}$$

$$= \underbrace{\sum_{n=0}^{\infty} \frac{(-1)^n}{(2n)!}\left(\frac{\pi}{4}\right)^{2n}}_{\text{even}} + \hat{O}\underbrace{\sum_{n=0}^{\infty} \frac{(-1)^n}{(2n+1)!}\left(\frac{\pi}{4}\right)^{2n+1}}_{\text{odd}}, \tag{4.45}$$

where the sum labeled 'even' corresponds to the terms with even n in the sum in eq. (4.40) and vice versa. Now, comparing with the Taylor series for the cosine function

$$\cos\theta = 1 - \frac{\theta^2}{2!} + \frac{\theta^4}{4!} - \frac{\theta^6}{6!} + ... \tag{4.46}$$

$$= \sum_{n=0}^{\infty} \frac{(-1)^n}{(2n)!}\theta^{2n}, \tag{4.47}$$

we see that for $\theta = \pi/4$, this is exactly the 'even'-sum of eq. (4.45). Intrigued by this crazy random happenstance, we calculate the series for $\sin\theta$:

$$\sin\theta = \theta - \frac{\theta^3}{3!} + \frac{\theta^5}{5!} - \frac{\theta^7}{7!} + ..., \tag{4.48}$$

$$= \sum_{n=0}^{\infty} \frac{(-1)^n}{(2n+1)!}\theta^{2n+1}, \tag{4.49}$$

which is equal to the 'odd' term if $\theta = \pi/4$. Having obtained these two series, we continue the calculation from (4.45):

$$\sum_{n=0}^{\infty} \frac{(-1)^n}{(2n)!}\left(\frac{\pi}{4}\right)^{2n} + \hat{O}\sum_{n=0}^{\infty} \frac{(-1)^n}{(2n+1)!}\left(\frac{\pi}{4}\right)^{2n+1} = \cos(\pi/4) + \hat{O}\sin(\pi/4), \tag{4.50}$$

$$= \frac{1}{\sqrt{2}} + \frac{1}{\sqrt{2}}\hat{O}, \tag{4.51}$$

which, in turn, gives us the end result:

$$\tau_i = \exp\left(\frac{\pi}{4}\gamma_{i+1}\gamma_i\right) = \frac{1}{\sqrt{2}}(1 + \gamma_{i+1}\gamma_i). \tag{4.52}$$

4.6 Matrix Form of Braiding Operators

In the presence of several vortices, the Majoranas can be combined in pairs to form complex fermions. The creation and annihilation operators of the fermions will then be represented by eqs. (3.8) and (3.9), respectively. The first fermion ($\hat{c}_1^\dagger$) will then be represented by γ_1 and γ_2, the second ($\hat{c}_2^\dagger$) by γ_3 and γ_4 and, generalizing, $\hat{c}_n^\dagger$ by γ_{2n-1} and γ_{2n}. This means that for odd values of i, the operator τ_i represents a braiding of two Majoranas that constitute the same fermion. For convenience, we will label the Majoranas γ_1 and γ_2 in the following, but the calculations presented hold for all odd i.

Using the expressions from eq. 3.10, normal ordering the operators $\hat{c}$ and $\hat{c}^\dagger$ ($\hat{c}^\dagger$ to the left, $\hat{c}$ to the right) and using the commutator from (3.2), we find

$$\tau_1 = \exp\left(\frac{\pi}{4}\gamma_2\gamma_1\right) = \exp\left(\frac{\pi}{4}i(\hat{c}^\dagger - \hat{c})(\hat{c}^\dagger + \hat{c})\right), \tag{4.53}$$

$$= \exp\left(-i\frac{\pi}{4}[\hat{c}, \hat{c}^\dagger]\right), \tag{4.54}$$

$$= \exp\left(i\frac{\pi}{4}(2\hat{c}^\dagger\hat{c} - 1)\right). \tag{4.55}$$

Choosing ($|0\rangle$, $\hat{c}^\dagger|0\rangle$) as a basis, τ_1 can the be expressed by a Pauli matrix, such that

$$\tau_1 = \exp\left(-i\frac{\pi}{4}\sigma_z\right), \tag{4.56}$$

where

$$-\sigma_z = \begin{pmatrix} -1 & 0 \\ 0 & 1 \end{pmatrix}. \tag{4.57}$$

Since the braiding of Majoranas constituting one fermion should leave the remaining fermions unchanged, we introduce the handy notation $\sigma_z^{(n)}$, which acts with the Pauli matrix on the

subspace of the n'th fermion only. In the case of two fermions and application of τ_1, for instance, we have

$$\tau_1 = \exp\left(-i\frac{\pi}{4}\sigma_z^{(1)}\right) = \exp\left(-i\frac{\pi}{4}\sigma_z \otimes \mathbb{1}\right). \tag{4.58}$$

Interfermionic braidings are best represented by eq. (4.34), such that for instance

$$\tau_2 = \frac{1}{\sqrt{2}}(1 + \gamma_3\gamma_2) = i(\hat{c}_2^\dagger\hat{c}_1^\dagger - \hat{c}_2\hat{c}_1 + \hat{c}_2\hat{c}_1^\dagger - \hat{c}_2^\dagger\hat{c}_1) + \mathbb{1}. \tag{4.59}$$

Note that when any matrix elements are calculated, the terms with a positive sign will turn negative as a result of the normal ordering.

Choosing a four-vortex system as an illustrative example, we express the three possible braiding operators in the basis $\{|0\rangle, \hat{c}_1^\dagger|0\rangle, \hat{c}_2^\dagger|0\rangle, \hat{c}_1^\dagger\hat{c}_2^\dagger|0\rangle\}$.

$$\tau_1 = \begin{pmatrix} e^{-i\pi/4} & & & \\ & e^{i\pi/4} & & \\ & & e^{-i\pi/4} & \\ & & & e^{i\pi/4} \end{pmatrix} = e^{-i\pi/4}\begin{pmatrix} 1 & & & \\ & i & & \\ & & 1 & \\ & & & i \end{pmatrix}, \tag{4.60}$$

$$\tau_3 = \begin{pmatrix} e^{-i\pi/4} & & & \\ & e^{-i\pi/4} & & \\ & & e^{i\pi/4} & \\ & & & e^{i\pi/4} \end{pmatrix} = e^{-i\pi/4}\begin{pmatrix} 1 & & & \\ & 1 & & \\ & & i & \\ & & & i \end{pmatrix}, \tag{4.61}$$

$$\tau_2 = \frac{1}{\sqrt{2}}\begin{pmatrix} 1 & 0 & 0 & -i \\ 0 & 1 & -i & 0 \\ 0 & -i & 1 & 0 \\ -i & 0 & 0 & 1 \end{pmatrix}. \tag{4.62}$$

The non-abelian braiding statistics of Majorana fermions can now be verified by checking that for instance $\tau_1\tau_2 \neq \tau_2\tau_1$.

Comparing the expressions for τ_1 and τ_3 with the general expression for a rotation operator from eq. (2.24), we see that these operators can only perform a rotation of $\pi/2$ around the z axis on the Bloch sphere, and thus can not constitute a universal set of single-qubit gates, as dicussed in section 2.6.

Also, the braiding operators can not be used to construct a CNOT gate as they are all parity conserving, i.e., they do not change the particle number from even to odd or vice versa. Why a parity mixing operator is neccesary to construct a CNOT gate is discussed in detail in section 6, so we will skip this subject for now and move on to describe a model that allows Bloch sphere rotations of arbitrary angles.

5 Non-Abelian Operations on Majorana Fermions

In this section we describe a recently proposed method [8] of carrying out braiding operations on a system of Majorana fermions. These manipulations will provide a richer set of single qubit operations than possible with the braiding operators derived in section 4.

5.1 Single Dot Coupled to One Majorana Fermion

The simplest version of the model, and hence our starting point, consists of two Majorana bound states, or MBSs, which together define a fermion M_{12}, as shown in figure 6. One MBS is tunnel coupled to a quantum dot which may contain N or $N+1$ electrons. Since each fermion can only be in the states $|0\rangle$ or $|1\rangle$, we know that the transfer of a single electron to or from a MBS will invert the parity of the fermion it defines. Thus we may invert the parity of M_{12} by forcing a charge transfer between the quantum dot and M_{12} by means of the gate $G1$.

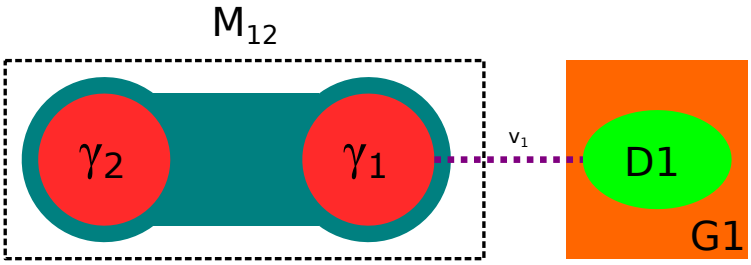

Figure 6: One Majorana fermion (γ_1) is tunnel coupled to the quantum dot ($D1$) by a tunnel coupling v_1. The gate $G1$ may cause an electron top tunnel between the dot and the fermionic system M_{12}. We denote this operation P_1

The quantum dot has two possible states containing N and $N+1$ electrons, respectively. Thus, we refer to the state $|\phi\rangle_D$ of the dot as either empty $|0\rangle_D$ or full $|1\rangle_D$. Since M_{12} is a fermionic system, we recall our discussion in section 3.1, and label its two states $|0\rangle_{M_{12}}$ and $|1\rangle_{M_{12}}$. Using the notation $|\psi\rangle \otimes |\phi\rangle = |\psi\rangle_{M_{12}}|\phi\rangle_D = |\psi\phi\rangle = |\Psi\rangle$, and denoting fermionic operators acting on the dot by $\hat{d}$ and $\hat{d}^\dagger$, we may then write our combined Hilbert space as

$$\begin{aligned}\mathcal{H} &= \{|00\rangle, |01\rangle, |10\rangle, |11\rangle\} \\ &= \{|0\rangle, \hat{d}^\dagger|0\rangle, \hat{c}^\dagger|0\rangle, \hat{d}^\dagger\hat{c}^\dagger|0\rangle\}.\end{aligned} \tag{5.1}$$

Now we would like to define a qubit by $\{|0\rangle, |1\rangle\}_{\text{qubit}} = \{|0\rangle_{M_{12}}, |1\rangle_{M_{12}}\}$.

Since we can not know the initial state of the fermionic Majorana system $|i\rangle_{M_{12}}$ without measuring on both γ_1 and γ_2 at the same time, we have to require degeneracy of the 'even' and 'odd' total parity states in order to use the Majorana system to represent a qubit with the computational basis states $\{|0\rangle, |1\rangle\}$ ({empty, full} fermion).

To examine the effects of the tunnel coupling, we add a 'tunneling term' H_{T_1} to the interaction Hamiltonian of the combined dot and Majorana system, which then becomes

$$H_1 = H_0 + H_{T_1} \tag{5.2}$$
$$= \varepsilon\hat{d}^\dagger\hat{d} + (v_1^*\hat{d}^\dagger - v_1\hat{d})\gamma_1 \tag{5.3}$$
$$= \varepsilon\hat{d}^\dagger\hat{d} + (v_1^*\hat{d}^\dagger - v_1\hat{d})(\hat{c} + \hat{c}^\dagger) \tag{5.4}$$

where ε is the ground state energy of the dot and v_1 is the tunnel coupling.

Our task is now to calculate all the matrix elements of this Hamiltonian. Starting with H_0, we see that the inner product $\langle\Psi_i|H_0|\Psi_j\rangle$ is zero if $\phi = 0$ or, from orthonormality, if $\psi_i \neq \psi_j$, so

$$\langle H_0\rangle = \delta_{\phi,1}\delta_{i,j}, \tag{5.5}$$

meaning that H_0 only gives us two nonzero matrix elements:

$$\langle 01|H_0|01\rangle = \langle 11|H_0|11\rangle = \varepsilon. \tag{5.6}$$

The tunnel Hamiltonian H_{T_1}, on the other hand, contains both the annihilation and creation operators of the dot and the Majorana state:

$$H_{T_1} = (v_1^*\hat{d}^\dagger - v_1\hat{d})(\hat{c} + \hat{c}^\dagger) \tag{5.7}$$
$$= v_1^*\hat{d}^\dagger\hat{c} - v_1\hat{d}\hat{c} + v_1^*\hat{d}^\dagger\hat{c}^\dagger - v_1\hat{d}\hat{c}^\dagger, \tag{5.8}$$

where we are going to evaluate the four terms separately. Fortunately, we can realize that each term only contribute with a single nonzero matrix element from the condition

$$0 = \hat{d}|0\rangle_D = \hat{d}^\dagger|1\rangle_D = \hat{c}|0\rangle_{M_{12}} = \hat{c}^\dagger|1\rangle_{M_{12}}, \tag{5.9}$$

and from the orthonormality of our basis states in (5.1).

As an example, consider the first term in eq. (5.8), $v_1^* \hat{d}^\dagger \hat{c}$. From the condition in (5.9), we see that the ket involved in calculating the nonzero element must be $|10\rangle$. From orthonormality, we then see that the corresponding bra must be $\left(\hat{d}^\dagger \hat{c}|10\rangle\right)^* = \langle 01|$, and thus we may finally calculate the matrix element:

$$\langle 01|v_1^* \hat{d}^\dagger \hat{c}|10\rangle = v_1^* \langle 0|\hat{d}\hat{d}^\dagger \hat{c}\hat{c}^\dagger|0\rangle \tag{5.10}$$

$$= v_1^* \langle 0|(1 - \hat{d}^\dagger \hat{d})(1 - \hat{c}^\dagger \hat{c})|0\rangle \tag{5.11}$$

$$= v_1^*, \tag{5.12}$$

where we have used that $\hat{c}\hat{c}^\dagger = 1 - \hat{c}^\dagger \hat{c}$, which follows from the anticommutator in (3.2). Reasoning this way, we can find all the terms in (5.8). Since we now know that $\langle 0|\hat{d}\hat{d}^\dagger \hat{c}\hat{c}^\dagger|0\rangle = 1$, we may simplify our calculations by rearranging the operators to this form. The anticommutation of fermionic operators then gives us a factor of minus one for each such permutation. So, we obtain

$$\langle 00|(-v_1 \hat{d}\hat{c})|11\rangle = -v_1 \langle 0|\hat{d}\hat{c}(\hat{d}^\dagger \hat{c}^\dagger|0\rangle) = -v_1(-1)\langle 0|\hat{d}\hat{d}^\dagger \hat{c}\hat{c}^\dagger|0\rangle = v_1, \tag{5.13}$$

$$\langle 11|v_1^* \hat{d}^\dagger \hat{c}^\dagger|00\rangle = v_1^*(\langle 0|\hat{c}\hat{d})\hat{d}^\dagger \hat{c}^\dagger|0\rangle = v_1^*(-1)^2 \langle 0|\hat{d}\hat{d}^\dagger \hat{c}\hat{c}^\dagger|0\rangle = v_1^*, \tag{5.14}$$

$$\langle 10|(-v_1)\hat{d}\hat{c}^\dagger|01\rangle = -v_1(\langle 0|\hat{c})\hat{d}\hat{c}^\dagger(\hat{d}^\dagger|0\rangle) = -v_1(-1)^3 \langle 0|\hat{d}\hat{d}^\dagger \hat{c}\hat{c}^\dagger|0\rangle = v_1. \tag{5.15}$$

In the 'even-odd total parity' basis $\{|0\rangle, \hat{d}^\dagger \hat{c}^\dagger|0\rangle, \hat{c}^\dagger|0\rangle, \hat{d}^\dagger|0\rangle\}$, the matrix representation of (5.4), then is a block diagonal matrix

$$H_1 = \begin{pmatrix} 0 & v_1 & 0 & 0 \\ v_1^* & \varepsilon & 0 & 0 \\ 0 & 0 & 0 & v_1 \\ 0 & 0 & v_1^* & \varepsilon \end{pmatrix}, \tag{5.16}$$

where the two diagonal blocks correspond to the even and odd total parity subspaces. Note that the total parity of the combined system is conserved, and that the 'even' $\{|0\rangle, \hat{d}^\dagger \hat{c}^\dagger|0\rangle\}$ and 'odd' $\{\hat{c}^\dagger|0\rangle, \hat{d}^\dagger|0\rangle\}$ subspaces behave identically. Thus, we may write the computational basis of the system from figure 6 as

$$\{|0\rangle, |1\rangle\}_{\text{qubit}} = \{|0\rangle_{M_{12}}, |1\rangle_{M_{12}}\}, \qquad \text{('even' total parity)}, \tag{5.17}$$

$$\{|0\rangle, |1\rangle\}_{\text{qubit}} = \{|1\rangle_{M_{12}}, |0\rangle_{M_{12}}\}, \qquad \text{('odd' total parity)}. \tag{5.18}$$

The energy eigenvalues are

$$\det(H_1 - \lambda \cdot \mathbb{1}) = 0 \Rightarrow \tag{5.19}$$

$$\lambda_\pm = \frac{\varepsilon \pm \sqrt{\varepsilon^2 + 4|v_1|^2}}{2}, \tag{5.20}$$

where we choose the lowest energy eigenvalue

$$E = \lambda_- = \varepsilon/2 - \sqrt{(\varepsilon/2)^2 + v_1^2}. \tag{5.21}$$

The degeneracy of the 'even' and 'odd' total parity subspaces allows us to use the fermionic Majorana system as our qubit despite the fact that we can not know in which subspace we operate in with the setup (figure 6). So initially, we have to describe the Majorana system in the superposition state of empty and full:

$$|i\rangle_{M_{12}} = \alpha|0\rangle_{M_{12}} + \beta(\hat{c}^\dagger|0\rangle)\rangle_{M_{12}}. \tag{5.22}$$

On the other hand, we are able to prepare the dot in a full charge state $|1\rangle_D = \hat{d}^\dagger|0\rangle_D$. The combined system is in the initial state: $|\Psi\rangle_i = |1\rangle_D|i\rangle_{M_{12}}$. Then, adiabatically changing the gate potential ε of the dot, we change the charge state of the dot, letting one electron tunnel

through to the Majorana system. The combined system is then described in the superposition state

$$|\Psi\rangle = a(\varepsilon)\cdot \hat{d}^\dagger|0\rangle_D\Big[\alpha|0\rangle_{M_{12}} + \beta(\hat{c}^\dagger|0\rangle)_{M_{12}}\Big] + b(\varepsilon)\cdot|0\rangle_D\Big[\alpha(\hat{c}^\dagger|0\rangle_{M_{12}}) + \beta|0\rangle_{M_{12}}\Big] \tag{5.23}$$

$$= a(\varepsilon)|1\rangle_D|i\rangle_{M_{12}} + b(\varepsilon)|0\rangle_D(\gamma_1|i\rangle_{M_{12}}), \tag{5.24}$$

where $b(\varepsilon)/a(\varepsilon) = E/v_1$. As we are able to control the coefficients $a(\varepsilon)$ and $b(\varepsilon)$ by changing ε we now let $\varepsilon/v_1 \to \infty$ inverting the parity of the Majorana system as $b(\varepsilon) \to 1$. This is defined as the tunnel-braid operation P_1:

$$|i\rangle_{M_{12}} \xrightarrow{P_1} \gamma_1|i\rangle_{M_{12}}. \tag{5.25}$$

Note that during the tunnel-braid operation P_1 our system is in the superposition state (5.23), but we end up with a product state of the dot and the Majorana system $|\Psi\rangle_f = |0\rangle_D|f\rangle_{M_{12}} = |0\rangle_D\gamma_1|i\rangle_{M_{12}}$. The Majorana is not entangled with the dot, which allows us to use the fermionic Majorana system to represent a qubit. Rewriting the operation (5.25) in terms of the transformation of the coefficients α, β, one realizes that the action of γ_1 corresponds to the Pauli $\hat{\sigma}_x$ gate

$$\begin{bmatrix} \alpha \\ \beta \end{bmatrix}_{M_{12}} \xrightarrow{P_1} \gamma_1 \begin{bmatrix} \alpha \\ \beta \end{bmatrix}_{M_{12}} = \begin{bmatrix} \beta \\ \alpha \end{bmatrix}_{M_{12}} = \hat{\sigma}_x \begin{bmatrix} \alpha \\ \beta \end{bmatrix}_{M_{12}}. \tag{5.26}$$

In general, coupling one Majorana to a quantum dot, we can perform the tunnel-braid operations

$$|i\rangle_{M_{12}} \xrightarrow{P_i} \gamma_i|i\rangle_{M_{12}}, \tag{5.27}$$

where $\gamma_{odd} = \hat{\sigma}_x$ and $\gamma_{even} = \hat{\sigma}_y$. In order to obtain a richer set of operations let us consider the case of two Majoranas coupled to a quantum dot.

Basic tunnel-braid operations in two-qubit basis

In the two-qubit computational basis $\{|00\rangle, |01\rangle, |10\rangle, |11\rangle\}$

$$\begin{aligned} \gamma_1 &= \begin{pmatrix} 0 & 0 & 1 & 0 \\ 0 & 0 & 0 & 1 \\ 1 & 0 & 0 & 0 \\ 0 & 1 & 0 & 0 \end{pmatrix}, \gamma_2 = \begin{pmatrix} 0 & 0 & -i & 0 \\ 0 & 0 & 0 & -i \\ i & 0 & 0 & 0 \\ 0 & i & 0 & 0 \end{pmatrix}, \\ \gamma_3 &= \begin{pmatrix} 0 & 1 & 0 & 0 \\ 1 & 0 & 0 & 0 \\ 0 & 0 & 0 & 1 \\ 0 & 0 & 1 & 0 \end{pmatrix}, \gamma_4 = \begin{pmatrix} 0 & -i & 0 & 0 \\ i & 0 & 0 & 0 \\ 0 & 0 & 0 & -i \\ 0 & 0 & i & 0 \end{pmatrix}. \end{aligned} \tag{5.28}$$

5.2 Several Majorana Fermions

In this section we investigate the effects of tunnel coupling two Majorana fermions, γ_1 and γ_2 to the same dot with v_1 and v_2, respectively. See figure 7.
In this case the interaction Hamiltonian (5.4) gets an extra term

$$H_{12} = H_0 + H_{T_1} + H_{T_2}, \tag{5.29}$$

where

$$H_{T_i} = (v_i^*\hat{d}^\dagger - v_i\hat{d})\gamma_i. \tag{5.30}$$

Using the previous method for calculating the matrix elements of H_{T_2} in the 'even-odd total parity' basis and remembering $\gamma_2 = i(\hat{c}^\dagger - \hat{c})$, we now find

$$H_{12} = \begin{pmatrix} 0 & v_1 - iv_2 & 0 & 0 \\ v_1 + iv_2 & \varepsilon & 0 & 0 \\ 0 & 0 & 0 & v_1 + iv_2 \\ 0 & 0 & v_1 - iv_2 & \varepsilon \end{pmatrix}. \tag{5.31}$$

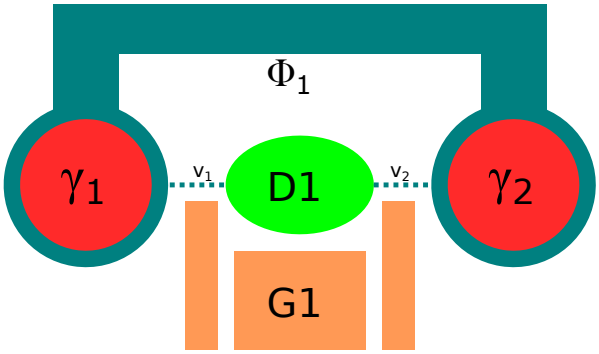

Figure 7: Two Majorana fermions (γ_1 and γ_2) are connected to the same dot ($D1$) through a tunnel coupling v_1 and v_2, respectively, controlled by gates next to $G1$. The tunnel-braid operation P_{12} can be applied using the gate $G1$. To obtain degeneracy of the 'even' and 'odd' total parity subspaces, we tune the phase difference of the Majoranas with a magnetic flux Φ_1 in the loop.

Now there is a phase difference between the 'even' and 'odd' energy eigenvalue

$$E_{\text{even or odd}} = \varepsilon - \sqrt{(\varepsilon/2)^2 + |v_1|^2 + |v_2|^2 \mp 2|v_1 v_2| \sin(\varphi_1/2)}, \tag{5.32}$$

where $\varphi_1 = 2\arg(v_1/v_2)$.

We need to restore the degeneracy of the 'even' and 'odd' subspaces in order to use the fermionic system as our qubit without any information about the system of Majoranas beforehand. This we can do by requiring

$$\sin(\varphi_1/2) = 0 \Rightarrow \varphi_1 = 2n\pi. \tag{5.33}$$

Since the phase difference can be controlled by a magnetic flux Φ_1 (see figure 7), so $\varphi_1 = \Phi_1/\Phi_0$, where $\Phi_0 = h/2e$, this can be done by tuning the magnetic flux to

$$\Phi_1 = 2n\pi \cdot \Phi_0 = \frac{hn\pi}{e}. \tag{5.34}$$

By this tuning, we obtain a Hamiltonian of the form (5.16) with $v_1 \to v$, where $v^2 = |v_1|^2 + |v_2|^2$ and

$$E_{\text{even or odd}} = \varepsilon - \sqrt{(\varepsilon/2)^2 + v^2}. \tag{5.35}$$

Additionally, we can define a new Majorana operator, obeying eqs. (3.16), as a linear superposition of our two Majoranas

$$\gamma_{12} = \frac{1}{v}(|v_1|\gamma_1 + |v_2|\gamma_2) = u\gamma_1 + v\gamma_2, \tag{5.36}$$

and a new dot-electron operator then cointaining a common phase

$$\widetilde{\hat{d}} = \hat{d}\exp[i\arg(v_1)]. \tag{5.37}$$

This allows us to rewrite the interaction Hamiltonian (5.29) as $H_{12} = H_0 + H_T$, where

$$H_T = v(\widetilde{\hat{d}}^\dagger + \widetilde{\hat{d}})\gamma_{12}. \tag{5.38}$$

At this point we have reduced the system of a dot coupled to two Majoranas to a dot coupled to a single superposition state of the two; γ_{12}. This allows us to carry out the same conclusions as in the previous section and define the tunnel-braid operation P_{12}:

$$\begin{aligned} |i\rangle_{M_{12}} \xrightarrow{P_{12}} \gamma_{12}|i\rangle_{M_{12}} &= (u\gamma_1 + v\gamma_2)|i\rangle_{M_{12}} \\ &= (u\hat{\sigma}_x + v\hat{\sigma}_y)|i\rangle_{M_{12}} \end{aligned} \tag{5.39}$$

In the following section, we describe these operations as rotations on the Bloch sphere.

5.2.1 Bloch Sphere Representation

Referring back to eq. (2.24) and neglecting a global phase of i, we see that the tunnel-braid operation of (5.39) is equivalent to a π-rotation of the Bloch vector around an axis in the xy-plane on the Bloch sphere:

$$iR_{\hat{n}_{xy}}(\pi) = i\left[\cos\left(\frac{\pi}{2}\right)\mathbb{1} - i\sin\left(\frac{\pi}{2}\right)(n_x\hat{\sigma}_x + n_y\hat{\sigma}_y)\right] \tag{5.40}$$

$$= n_x\hat{\sigma}_x + n_y\hat{\sigma}_y \tag{5.41}$$

$$= \gamma_{12} \tag{5.42}$$

with $u = n_x$ and $v = n_y$. We are able to tune u and v and this way perform π-rotations around an arbitrary axis in the xy-plane. We may also apply subsequent operations, which we write as

$$|i\rangle_{M_{12}} \xrightarrow{P_{12}} \gamma_{12}|i\rangle_{M_{12}} \xrightarrow{P'_{12}} \gamma'_{12}\gamma_{12}|i\rangle_{M_{12}}, \tag{5.43}$$

which corresponds to the action of the product $\gamma'_{12}\gamma_{12}$ onto the initial state. In terms of the tuneable coefficients, the operator product is

$$\gamma'_{12}\gamma_{12} = (u'u + v'v) + (u'v\gamma_1\gamma_2 + v'u\gamma_2\gamma_1) \tag{5.44}$$

$$= (u'u + v'v) + i(u'v - v'u)\hat{\sigma}_z \tag{5.45}$$

$$= -\left[\cos(\phi/2)\mathbb{1} - i\sin(\phi/2)\hat{\sigma}_z\right] \tag{5.46}$$

$$= -R_{\hat{n}_z}(\phi). \tag{5.47}$$

This is a rotation by a tunable angle around the z-axis on the Bloch sphere as visualized in figure 8. Applying a third operation P''_{12} we are again able to express the sequence of tunnel-

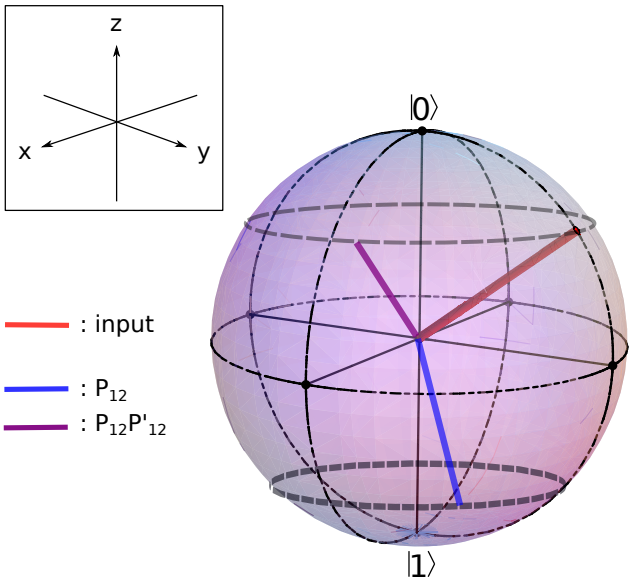

Figure 8: Visualization of rotation induced by P_{12} and $P_{12}P'_{12}$ operation on the Bloch sphere.
(1) Take the blue vector as the initial qubit state, then applying a operation P_{12} makes the vector rotate π around the corresponding axis in the xy-plane and transforms to the red state vector.
(2) Applying a second P'_{12} operation with different coefficients rotates then the red vector into the purple. We see that the differense between the blue and the purple vector is just a rotation by some angle around the z-axis.

braid operations as a π-rotation around an axis in the xy-plane, so we are basically back to our starting point.

With the Bloch sphere representation in mind we see that an odd sequence of P_{12} operations induces a π-rotation around an tuneable axis in the xy-plane and an even sequence induces a rotation by tunable angle around the z-axis.

To summarize, in the system of figure 7 we are restricted to operations that induce two types of rotations on the Bloch sphere; a rotation by π around a tunable axis in the xy-plane and a rotation by tuneable angle around a z-axis. Since we can not decompose the general rotation operator (2.24) into these operations, they do not constitute a universal set of single-qubit operations. Note that a qubit is composed of two Majorana fermions.

5.2.2 Four Majoranas Representing a Qubit

Consider now a system of four Majoranas coupled to quantum dots as shown in figure 9. Now we have three tunnel-braiding operation P_{12}, P_{23} and P_{34} of superposition modes avaible. The

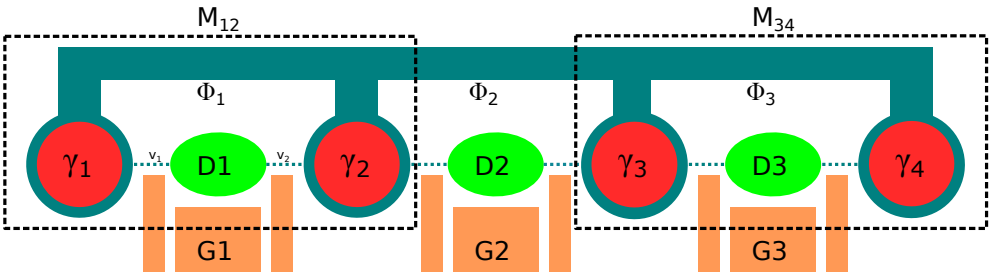

Figure 9: Four Majorana states $\gamma_1, \gamma_2, \gamma_3, \gamma_4$ coupled to quantum dots D1, D2 and D3.

matrix representation of two subsequent tunnel-braiding operations $P_{12}P'_{12}$ on the same dot with different coupling is in the 'even-odd' parity basis $\{|00\rangle, |11\rangle, |01\rangle, |10\rangle\}$:

$$\gamma_{12}\gamma'_{12} = \begin{pmatrix} & & & a-ib \\ & & a+ib & \\ & a-ib & & \\ a+ib & & & \end{pmatrix} \begin{pmatrix} & & & a'-ib' \\ & & a'+ib' & \\ & a'-ib' & & \\ a'+ib' & & & \end{pmatrix} \tag{5.48}$$

$$= \begin{pmatrix} (a-ib)(a'+ib') & & & \\ & (a+ib)(a'-ib') & & \\ & & (a-ib)(a'+ib') & \\ & & & (a+ib)(a'-ib') \end{pmatrix}. \tag{5.49}$$

If we instead perform the operations on the second fermion, i.e. $P'_{23}P_{23}$, this yields the same result as $\gamma_{12}\gamma'_{12} = [\gamma_{34}\gamma'_{34}]^T$. Applying two subsequent interchange tunnel-braidings P_{23} on the other hand yields

$$\gamma_{23}\gamma'_{23} = (u\hat{\sigma}_y^{(1)} + v\hat{\sigma}_x^{(2)})(u'\hat{\sigma}_y^{(1)} + v'\hat{\sigma}_x^{(2)}) \tag{5.50}$$

$$= \begin{pmatrix} 0 & 0 & c & -id \\ 0 & 0 & id & c \\ c & -id & 0 & 0 \\ id & c & 0 & 0 \end{pmatrix} \begin{pmatrix} 0 & 0 & c' & -id' \\ 0 & 0 & id' & c' \\ c' & -id' & 0 & 0 \\ id' & c' & 0 & 0 \end{pmatrix} \tag{5.51}$$

$$= \begin{pmatrix} cc'+dd' & -i(dc'+cd') & 0 & 0 \\ i(dc'+cd') & cc'+dd' & 0 & 0 \\ 0 & 0 & cc'+dd' & -i(dc'+cd') \\ 0 & 0 & i(dc'+cd') & cc'+dd' \end{pmatrix}. \tag{5.52}$$

These block diagonal matrices have only parity conserving elements and the 'even' and 'odd' subspaces are degenerate, since their matrix elements are identical. This allow us to choose the

'even' parity basis $\{|00\rangle, |11\rangle\}$ and only consider the matrix representations of the tunnel-braid operations in this supspace.

Acting with two operations on one fermion we find an operation equivalent to a rotation by tuneable angle around the z-axis:

$$\gamma_{12}\gamma'_{12} = \begin{pmatrix} aa' + bb' + i(ab' - ba') & 0 \\ 0 & aa' + bb' + i(-ab' + ba') \end{pmatrix} \tag{5.53}$$

$$= (aa' + bb')\mathbb{1} + i(ab' - ba')\hat{\sigma}_z \tag{5.54}$$

$$= -R_{\hat{n}_z}(\phi) \tag{5.55}$$

Furthermore, two interfermionic operations are a rotation by tunable angle around the y-axis[4]

$$\gamma_{23}\gamma'_{23} = \begin{pmatrix} vv' + uu' & -i(uv' + uv') \\ i(uv' + vu') & vv' + uu' \end{pmatrix} \tag{5.56}$$

$$= (vv' + uu')\mathbb{1} + (uv' + uv')\hat{\sigma}_y \tag{5.57}$$

$$= -\left[\cos(\phi/2)\mathbb{1} - i\sin(\phi/2)\hat{\sigma}_y\right] \tag{5.58}$$

$$= -R_{\hat{n}_y}(\phi). \tag{5.59}$$

Having obtained a set of operations that makes us capable of rotations by arbitrary angle around two non-parallel rotation axis, we have in fact obtained a universal set of single qubit operations.

6 Discussion & Conclusion

The aim of this section is to discuss possible alterations to the model described in section 5 and to present our conclusions.

6.1 Discussion

Although the model discussed in section 5 provides a complete set of single-qubit operations, a controlled two-qubit gate is needed to allow for universal quantum computation. Unfortunately, we have not been able to remedy this, but we will discuss here two modifications that we have considered to the model in question. One modification introduces an 'auxiliary qubit', whereas the other involves redefining the computational basis.

6.1.1 Auxiliary Qubits

The main concern which lead us to consider this modification is the inability of the possible tunnel-braid operations to mix parity conserving with parity changing operations. To clarify, consider an arbitrary matrix M:

$$M = \begin{pmatrix} M_{11} & M_{12} & M_{13} & M_{14} \\ M_{21} & M_{22} & M_{23} & M_{24} \\ M_{31} & M_{32} & M_{33} & M_{34} \\ M_{41} & M_{42} & M_{43} & M_{44} \end{pmatrix}. \tag{6.1}$$

In the computational basis of section 5.2, the blue matrix elements conserve parity, whereas the red elements change parity. This is more easily identified in Dirac notation where parity changing operations in general contain terms like

$$\begin{aligned} M_{ij} &\propto |\text{even}\rangle\langle\text{odd}|, \quad \text{or} \\ M_{ij} &\propto |\text{odd}\rangle\langle\text{even}|. \end{aligned} \tag{6.2}$$

[4] In [?] $P_{23}P'_{23}$ correspond to a rotaion around the x-axis. This operator product correspond to our $P_{13}P'_{13}$ operation.

For instance the M_{12} term becomes $M_{12} \cdot |11\rangle\langle 01|$. Since the ket and bra have even and odd total parity, respectively, the M_{12} term is parity changing. Comparing the matrix in (6.1) with the CNOT

$$\begin{pmatrix} 1 & 0 & 0 & 0 \\ 0 & 1 & 0 & 0 \\ 0 & 0 & 0 & 1 \\ 0 & 0 & 1 & 0 \end{pmatrix}, \tag{6.3}$$

we see that the operation corresponding to the CNOT gate must mix parity changing and conserving terms. This is a problem because we see from (5.28) that the fundamental tunnel-braiding operations available to us (γ_1 to γ_4) are all parity changing, meaning that also linear superpositions will be parity changing. Note also that even though we may apply consecutive operations, it follows from (6.2) that this will only affect the total change of parity for the operator and not mix parities.

One way to attempt to resolve this is to introduce an auxiliary qubit, as shown in figure 10. Including this new fermion composed of γ_5 and γ_6, the Hilbert space becomes

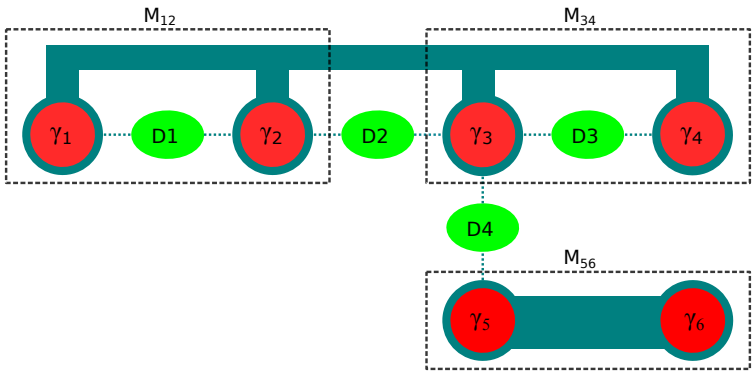

Figure 10: An additional dot couples one of the two fermions constituting the computational basis with an auxiliary qubit, which is not part of the computational basis.

$$\mathcal{H} = \{|000\rangle, |001\rangle, |010\rangle, |011\rangle, |100\rangle, |101\rangle, |110\rangle, |111\rangle\}. \tag{6.4}$$

This makes a few additional tunnel-braiding operations possible, such as a quantum dot coupling to γ_3 and γ_5 with coupling strengths a and b, respectively, which we may write as

$$\gamma_{35} = a \cdot \hat{\sigma}_x^{(2)} + b \cdot \hat{\sigma}_x^{(3)} \tag{6.5}$$

$$\tag{6.6}$$

However, if we restrict ourselves to the subspace of the Hilbert space constituted by the old computational basis, this operation is equivalent to $\mathbb{1} \otimes (a \cdot \mathbb{1} + b \cdot \hat{\sigma}_x)$ and thus has the matrix representation

$$\gamma_{35} = \begin{pmatrix} a & b & 0 & 0 \\ b & a & 0 & 0 \\ 0 & 0 & a & b \\ 0 & 0 & b & a \end{pmatrix}, \tag{6.7}$$

which at first sight appears to solve the problem. However, the representation of γ_{35} in the computational basis is not unitary $\gamma_{35}^\dagger \gamma_{35} \neq \mathbb{1}$, rendering the general theory of quantum information inapplicable. Of course the transformation is unitary in the basis of the complete Hilbert space where an entangled state is created – Letting i and f denote initial and final states of individual fermions, we may write

$$\gamma_{35}|iii\rangle = |i\rangle_1 \left(a|i\rangle_2|f\rangle_3 + b|f\rangle_2|i\rangle_3\right), \tag{6.8}$$

but to restore unitarity, we must perform a measurement on fermion 2 or three. Any desired superposition state achieved by this parity mixing operation is thus collapsed, and we are thus no better off than we started.

6.1.2 Change of Computational Basis

As described in section 2.2, the only condition necessary to describe a qubit is a two-dimensional complex vector. Recalling the Hilbert space of eq. (5.1), we see that nothing in fact prevents us from defing our qubits in a basis other than $\{|0\rangle_1, |1\rangle_1\}, \{|0\rangle_2, |1\rangle_2\}$. For example, we may define our qubits in bases with distinct parity. Denoting qubit numbers by subscript, we define

$$\begin{aligned} \{0,1\}_1 &\equiv \{|00\rangle, |11\rangle\}, \\ \{0,1\}_2 &\equiv \{|01\rangle, |10\rangle\}. \end{aligned} \tag{6.9}$$

In this computational basis, the fundamental tunnel-braid operations become

$$\gamma_1 = \begin{pmatrix} 0 & 0 & 0 & 1 \\ 0 & 0 & 1 & 0 \\ 0 & 1 & 0 & 0 \\ 1 & 0 & 0 & 0 \end{pmatrix}, \gamma_2 = \begin{pmatrix} 0 & 0 & 0 & -i \\ 0 & 0 & i & 0 \\ 0 & -i & 0 & 0 \\ i & 0 & 0 & 0 \end{pmatrix}, \tag{6.10}$$

$$\gamma_3 = \begin{pmatrix} 0 & 0 & 1 & 0 \\ 0 & 0 & 0 & 1 \\ 1 & 0 & 0 & 0 \\ 0 & 1 & 0 & 0 \end{pmatrix}, \gamma_4 = \begin{pmatrix} 0 & 0 & -i & 0 \\ 0 & 0 & 0 & i \\ i & 0 & 0 & 0 \\ 0 & -i & 0 & 0 \end{pmatrix}. \tag{6.11}$$

In this basis, it is actually possible to construct a controlled phase gate:

$$\frac{1}{2}\gamma_1\gamma_4\left(\gamma_1+\gamma_2\right)\left(\gamma_3+\gamma_4\right) = \begin{pmatrix} 1 & 0 & 0 & 0 \\ 0 & 1 & 0 & 0 \\ 0 & 0 & i & 0 \\ 0 & 0 & 0 & -i \end{pmatrix}, \tag{6.12}$$

which seems very promising at first sight. Unfortunately, it can be seen from the definition of the new computational basis in (6.9) that since the states of both qubits comprise states of both fermions, any change to the state of an individual fermion will change the state of both qubits. In other words, *single-qubit operations are not possible in the computational basis descriped by* (6.9).

6.2 Conclusion

In this thesis, we gave a brief introduction to the subject of quantum computation, and the theory of Majorana fermions. Using only basic quantum mechanics, we found the effects of flux quantization and the Aharonov-Bohm phase, and finally derived the non-abelian statistics of Majorana fermions realized in vortices in p-wave superconductors.

After arguing that the braiding of said Majorana fermions could never constitute a universal set of quantum gates, we moved on to consider af model that utilized tunnel-braid operations to perform Bloch sphere rotations of arbitrary angles. We found that it was possible to obtain a universal set of single-qubit gates if we exploited the degeneracy of the even and odd parity subspaces by representing a qubit with four Majorana fermions. This lead us to investigate whether it was also possible to construct a controlled gate.

This was only possible by defining the two qubits in distinct parity subspaces, which in turn prevented us from performing single-qubit operations and thus forced us to abandon the computational basis that defined qubits in seperate parity subspaces.

We also identified the absence of parity mixing matrix elements in the tunnel-braiding operators as an obstruction to our attempts to construct a controlled gate. We attempted to remedy this by introducing an auxiliary qubit, which was not included in the computational basis. However, this violated the unitarity requirement of gates in quantum information theory. As we saw no way of restoring this unitarity without destroying the entanglement associated with controlled gates, we also gave up the scheme involving auxiliary qubits.

Of course, we have not shown that it is not possible to construct a universal set of gates with the model in question, but we have showed that the task is not straightforward and demonstrated the limitations of the physical model with different computational bases.

References

[1] Michael A. Nielsen and Isaac L. Chuang, *Quantum Computation and Quantum Information*, Cambridge University Press (2000)

[2] P. Phillips, *Advanced Solid State Physics*, Westview Press, 2003

[3] D. A. Ivanov, *Non-Abelian Statistics of Half-Quantum Vortices in p-Wave Superconductors*, Phys. Rev. Lett. 86, 268 (2001)

[4] Charles Kittel, *Introduction to Solid State Physics*, 7th edition, John Wiley and Sons, Inc.(1996)

[5] James F. Annett, *Superconductivity, Superfluids and Condensates*, Oxford University Press (2004)

[6] K.F. Riley, M.P. Hobson and S.J. Bence, *Mathematical Methods for Physics and Engineering*, Cambridge University Press (2006)

[7] Ady Stern, *Anyons and the quantum Hall effect — A pedagogical review*, Annals of Physics 323 (2008) 204–249

[8] Karsten Flensberg, *Non-Abelian Operations on Majorana Fermions via Single-Charge Control*, Phys. Rev. Lett. 106, 090503 (2011)